◆ Human Brain Mapping 35:4180–4192 (2014) ◆

Intranetwork and Internetwork Functional Connectivity Abnormalities in Pediatric Multiple Sclerosis

Maria A. Rocca,[1,2] Paola Valsasina,[1] Martina Absinta,[1,2] Lucia Moiola,[2] Angelo Ghezzi,[3] Pierangelo Veggiotti,[4] Maria P. Amato,[5] Mark A. Horsfield,[6] Andrea Falini,[7,8] Giancarlo Comi,[2] and Massimo Filippi[1,2]*

[1]*Neuroimaging Research Unit, Institute of Experimental Neurology, Division of Neuroscience, San Raffaele Scientific Institute, Vita-Salute San Raffaele University, Milan, Italy*
[2]*Department of Neurology, San Raffaele Scientific Institute, Vita-Salute San Raffaele University, Milan, Italy*
[3]*Multiple Sclerosis Study Center, Department of Neurology, Hospital of Gallarate, Gallarate, Italy*
[4]*Child Neuropsychiatry Unit, Fondazione "Istituto Neurologico Casimiro Mondino", Pavia, Italy*
[5]*Department of Neurology, University of Florence, Florence, Italy*
[6]*Department of Cardiovascular Sciences, University of Leicester, Leicester, United Kingdom*
[7]*Department of Neuroradiology, San Raffaele Scientific Institute, Vita-Salute San Raffaele University, Milan, Italy*
[8]*CERMAC, Division of Neuroscience,San Raffaele Scientific Institute, Vita-Salute San Raffaele University, Milan, Italy*

Abstract: Active motor functional magnetic resonance imaging (fMRI) studies have shown that pediatric multiple sclerosis (MS) patients have a strictly lateralized pattern of activations and a preserved functional connectivity (FC) within the motor system when compared to age-matched healthy controls. However, it is still not clear whether a preserved FC in pediatric MS is present only in the motor system, or involves other relevant functional system. Resting-state (RS) fMRI is a valuable tool for an unbiased investigation of FC abnormalities of multiple networks. This study explored abnormalities of RS FC within and between large-scale neuronal networks from 44 pediatric MS patients and 27 controls and their correlation with clinical, neuropsychological, and conventional MRI measures. Compared to controls, pediatric MS patients had a decreased FC of several regions of the sensorimotor, secondary visual, default-mode (DMN), executive control, and bilateral working memory (WMN) networks. They also experienced an increased FC in the right medial frontal gyrus of the attention network, which was correlated with *T*2 lesion volume. Cognitively impaired patients had decreased RS FC of the right precuneus of the left WMN. An increased FC between the sensorimotor network and the DMN, and between the L WMN and the attention network as well as a decreased FC between L WMN and the DMN were also found. A distributed pattern of FC abnormalities within large-scale

Contract grant sponsor: Italian Ministry of Health; Contract grant number: GR-2009-1529671.

*Correspondence to: Massimo Filippi, Neuroimaging Research Unit, Institute of Experimental Neurology, Division of Neuroscience, San Raffaele Scientific Institute, Vita-Salute San Raffaele University, Milan, Italy. E-mail: m.filippi@hsr.it

Received for publication 28 August 2013; Revised 27 November 2013; Accepted 7 January 2014.

DOI 10.1002/hbm.22469
Published online 7 February 2014 in Wiley Online Library (wileyonlinelibrary.com).

neuronal networks occurs in pediatric MS patients, contributes to their cognitive status, and is partially driven by focal white matter lesions. Internetwork connectivity is relatively preserved in these patients. *Hum Brain Mapp 35:4180–4192, 2014.*

Key words: pediatric multiple sclerosis; resting state functional connectivity; large-scale networks; lesions; diffusion tensor MRI; disability

INTRODUCTION

An estimated 3–10% of patients with multiple sclerosis (MS) have an onset of the disease before the age of 18 years [Banwell et al., 2007; Krupp et al., 2007]. Compared to their adult counterparts, patients with pediatric-onset MS take longer to accrue similar levels of disability although they tend to reach a certain level of disability at a younger age than adult-onset MS patients [Renoux et al., 2007; Simone et al., 2002].

Several factors have been examined to explain the more favorable clinical outcome of patients with pediatric MS, at least in the short and medium terms, including their immunological profile [Chabas et al., 2010], the level of myelination of the CNS [Absinta et al., 2011; Ghassemi et al., 2008], which might lead to a different susceptibility to disease-related structural damage, and a preservation of their functional reserve because of brain plasticity. Although several investigations have been performed to clarify the first two aspects, at present only two studies have assessed brain functional reorganization in this patient population [Rocca et al., 2009, 2010a]. Both of these studies used fMRI with an active paradigm to explore motor system function in terms of activations and functional connectivity (FC). They found that, in contrast to adult patients with relapsing remitting (RR) MS who showed a bilateral recruitment of several regions of the sensorimotor network, pediatric RRMS patients experienced a focused and strictly lateralized pattern of movement-associated brain activations, with increased fMRI activity only of the contralateral primary sensorimotor cortex when compared to age-matched healthy controls [Rocca et al., 2009, 2010a]. No [Rocca et al., 2010a] or minimal modifications [Rocca et al., 2009] of motor network FC were found in these patients. Whether this behavior is limited to the motor system in the pediatric population or, conversely, involves the functional organization of the brain more globally has not yet been determined. Clearly, one of the main issues related to the use of active fMRI paradigms, especially in pediatric and diseased populations, is that the results can be influenced by task performance. Recently, a task-free approach, based on the quantification of FC among anatomically separate, but functionally related brain regions at rest has been introduced. Resting-state (RS) fMRI is markedly improving our knowledge of different psychiatric and neurological conditions, including MS [Bonavita et al., 2011; Hawellek et al., 2011; Rocca et al., 2010b; Roosendaal et al., 2010], and might be also useful to obtain an unbiased investigation of FC abnormalities of multiple networks. RS FC has not been employed in pediatric patients with MS so far.

In this study, we investigated the integrity of the principal brain RS networks (RSNs) and interactions among these networks in a relatively large sample of right-handed pediatric RRMS patients. To this aim, we performed, in addition to a "classical" analysis of RS FC, a functional network connectivity (FNC) analysis. The correlations between abnormalities of intra- and internetwork connectivity and clinical (disease duration, disability, and cognitive impairment) and MRI measures of structural damage (*T*2 lesions and microscopic damage to the normal-appearing white matter and gray matter [GM]) were also explored.

METHODS

Subjects

We studied 44 consecutively recruited right-handed [Oldfield, 1971] pediatric patients with RRMS [Lublin and Reingold, 1996], and 27 gender- and age-matched healthy controls, with no previous history of neurological or psychiatric disorders, and a normal neurological exam (Table I). Patients with acute disseminated encephalomyelitis were excluded in accordance with published operational criteria [Dale et al., 2009; Krupp et al., 2007]. To be included, patients had to be relapse- and steroid-free for at least 3 months. Exclusion criteria were concomitant therapy with antidepressants, psychoactive drugs, and a history of major medical, neurological or psychiatric disorders as well as drug and alcohol abuse.

Ethics Committee Approval

Approval was received from the local ethical standards committee on human experimentation, and written informed consent was obtained from all subjects' parents prior to study enrolment.

Neuropsychological Evaluation

All patients underwent a neuropsychological assessment using the Brief Neuropsychological Battery for Children (BNBC), which has been standardized and validated for

TABLE I. Main demographic, clinical, and structural MRI characteristics of the control subjects and pediatric patients with MS, first considered as a whole and then divided into cognitively preserved (CP) and cognitively impaired (CI) MS patients

	Healthy controls	Pediatric MS patients	CP MS patients	CI MS patients	*P*-value[a]	*P*-value[b]
Boys/girls	11/16	16/28	9/19	7/9	0.7	0.7
Mean age (years) (range)	15.3 (9.4–18)	15.1 (7.6–18)	15.0 (11–18)	15.1 (7.6–18)	0.5	0.7
Median EDSS (range)	—	1.5 (0.0–4.0)	1.0 (0.0–2.5)	1.5 (0.0–4.0)	—	0.4
Mean disease duration (years) (range)	—	1.9 (0.5–8.1)	1.4 (0.5–4.9)	2.8 (0.5–8.1)	—	0.03
Mean brain *T*2 LV (mL) (SD)	—	4.8 (6.7)	3.0 (2.1)	7.6 (10.1)	—	0.2
Mean BPF (%) (SD)	0.85 (0.01)	0.84 (0.01)	0.84 (0.01)	0.83 (0.01)	0.10	0.09
Mean white matter fraction (%) (SD)	0.35 (0.01)	0.35 (0.01)	0.35 (0.01)	0.34 (0.01)	0.9	0.3
Mean GMF (%) (SD)	0.50 (0.01)	0.49 (0.01)	0.49 (0.01)	0.49 (0.01)	0.12	0.3
Average lesion FA (SD)	—	0.33 (0.03)	0.33 (0.03)	0.33 (0.03)	—	0.8
Average lesion MD (mm^2/s^{-1}) (SD)	—	1.01 (0.08)	1.01 (0.09)	1.02 (0.04)	—	0.09
Mean normal-appearing white matter FA (SD)	0.41 (0.02)	0.38 (0.03)	0.39 (0.02)	0.36 (0.03)	<0.001	<0.001
Mean normal-appearing white matter MD (mm^2/s^{-1}) (SD)	0.79 (0.02)	0.79 (0.02)	0.79 (0.01)	0.80 (0.04)	0.9	0.3
Mean GM MD (mm^2/s^{-1}) (SD)	0.87 (0.02)	0.89 (0.03)	0.89 (0.02)	0.90 (0.04)	0.03	0.04
Mean GM FA (SD)	0.17 (0.01)	0.17 (0.02)	0.17 (0.01)	0.18 (0.02)	0.7	0.6

[a]Mann–Whitney *U*-test.
[b]Kruskall and Wallis test.
Abbreviations: EDSS, expanded disability status scale; LV, lesion volume; BPF, brain parenchymal fraction; GMF, gray matter fraction; FA, fractional anisotropy; MD, mean diffusivity; GM, gray matter.

Italian pediatric MS patients [Portaccio et al., 2009]. The assessment was performed within 3 days of the MRI study by an experienced observer blinded to the clinical and MRI results. The BNBC includes: (a) global cognitive functioning with intelligence quotient; (b) verbal learning and delayed recall with the Selective Reminding Test (SRT, SRT-Delayed); (c) visuospatial learning and delayed recall with the Spatial Recall Test (SPART, SPART-Delayed); (d) sustained attention and concentration with the Symbol Digit Modalities Test (SDMT) and the Trail Making Test (TMT-A and TMT-B); (e) abstract reasoning through the Modified Card Sorting Test; (f) expressive language through a Semantic and Phonemic verbal fluency test and an Oral Denomination test; and (g) receptive language using the Token test, the Indication of Pictures from the Neuropsychological Examination for Aphasia, and the Phrase Comprehension test from the Battery for the Analysis of Aphasic Deficits. The 5th or 95th percentile of the corrected scores of the normative data was used as the cut-off for determining failure at a given test. Patients with an abnormal performance in $\geq$2 tests were classified as cognitively impaired (CI) [Portaccio et al., 2009].

MRI Acquisition

Using a 3.0 Tesla Philips Intera scanner, the following images of the brain were acquired from all subjects: (a) T_2^*- weighted single-shot echo planar imaging (EPI) sequence for RS fMRI (repetition time [TR] = 3,000 ms, echo time [TE] = 35 ms, flip angle [FA] = 90°, field of view [FOV] = 240 mm × 240 mm; matrix = 128 × 128, slice thickness = 4 mm, 200 sets of 30 contiguous axial slices, parallel to the AC–PC plane); (b) dual-echo turbo spin echo (SE) (TR/TE = 3,500/24,120 ms; FA = 150°; FOV = 240 mm × 240 mm; matrix = 256 × 256; echo train length = 5; 44 contiguous, 3-mm-thick axial slices); (c) 3D T1-weighted fast field echo (FFE) (TR = 25 ms, TE = 4.6 ms, FA = 30°, FOV = 230 mm^2, matrix = 256 × 256, slice thickness = 1 mm, 220 contiguous axial slices, in-plane resolution = 0.89 × 0.89 mm^2); and (d) pulsed-gradient SE EPI (TR/TE = 8,775/58 ms, acquisition matrix = 112 × 88, FOV = 240 × 231 mm^2, 55 contiguous, 2.3-mm thick, axial slices) with SENSE (acceleration factor = 2), and diffusion gradients applied in 35 noncollinear directions. Two optimized b factors were used for acquiring diffusion weighted images (b = 0 and b = 900 s mm^{-2}). Total acquisition time for RS fMRI was about 10 min. During scanning, subjects were instructed to remain motionless, to close their eyes, and not to think anything in particular. All subjects reported that they had not fallen asleep during scanning, according to a questionnaire filled out immediately after the MRI session.

Analysis of Intrinsic Brain FC in RSNs

Using SPM8, RS fMRI scans were realigned to the first one of each session using a six-degree (three translations and three rotations) rigid-body transformation to correct for minor head movements. The mean cumulative translations were 0.20 mm (standard deviation [SD] = 0.15 mm)

for controls and 0.26 mm (SD = 0.20 mm) for pediatric MS patients ($P = 0.4$), the mean rotations were $<0.3°$ in both groups ($P = 0.6$). The mean individual motion was calculated for each subject as the average of the six realignment parameters estimated by SPM. Data were then normalized to the SPM8 default EPI template using a standard affine transformation, with data subsampling to a resolution of 3 mm × 3 mm × 4 mm [Calhoun et al., 2001], and smoothing using a 3D 6-mm Gaussian kernel. We decided to use the default EPI template provided by SPM, because normalization to this template was demonstrated to work well on subjects older than 6 years, which was the case of our study [Muzik et al., 2000]. The goodness of normalization was confirmed by the high correlation found between the normalized images and the default EPI template (r-values ranging from 0.95 to 0.97). Linear detrending and band-pass filtering between 0.01 and 0.08 Hz were performed using the REST software (http://resting-fmri.sourceforge.net/) to partially remove low-frequency drifts and physiological high-frequency noise.

After these preprocessing steps, RS FC was assessed using an independent component analysis (ICA) with the GIFT software [Calhoun et al., 2001], and following three main steps: (i) data reduction, (ii) group ICA, and (ii) back reconstruction. First, individual subjects' data were reduced to a lower dimensionality by using a principal component analysis. Then, RS fMRI data from all subjects were concatenated and reduced to one group. The independent group components were estimated using the Infomax approach [Bell and Sejnowski, 1995] and were used to compute spatial maps and temporal profiles of the individual subject components (back reconstruction). The number of independent group components was 40, a dimension determined using the minimum description length criterion [Calhoun et al., 2001]. The statistical reliability of the IC decomposition was tested by using the ICASSO toolbox [Himberg et al., 2004], and by running Infomax 10 times with different initial conditions and bootstrapped data sets. Individual functional maps were converted to Z-scores before entering group statistics, to obtain voxel values comparable across subjects.

Visual inspection of the spatial patterns and a frequency analysis of the spectra of the estimated ICs allowed the removal of components clearly related to artifacts. A systematic process was also applied to inspect and select the components of interest from those remaining. To identify ICs with potential functional relevance, a frequency analysis of the IC time courses was first performed to detect those with a high (50% or greater) spectral power at a low frequency (between 0.01 and 0.05 Hz). Then, RSNs of interest were selected using spatial correlation against a set of a priori defined network templates. We chose to use standard templates for the detection of RSNs because of the relatively high mean age of our study population (i.e., 15 years for both controls and pediatric MS patients). Indeed, it has been recently shown that, by the age of 10–12 years, only small spatial differences from adult patterns are present in all RSNs with functional relevance [Jolles et al., 2011; Supekar et al., 2010]. The default-mode network (DMN) was identified through a voxel-wise correlation with the DMN template provided in GIFT [Franco et al., 2009]. The remaining network templates were generated using the WFU Pickatlas [Maldjian et al., 2003] on the basis of the Brodmann areas and cluster peaks reported in the literature (salience network [SN]: [Seeley et al., 2007]; frontoparietal working memory networks [WMN], lateralized to the left and right hemisphere: [Damoiseaux et al., 2006]; executive control [ECN], sensorimotor, primary visual, secondary visual and auditory networks: [Smith et al., 2009]; frontoparietal attention network: [Fox et al., 2005]). The ICs with the highest square correlation coefficients (R^2, as implemented in GIFT the software package) with each of these templates were selected. Only components having a square correlation coefficient of >0.20 (corresponding to a plain correlation coefficient of >0.40) were included in the analysis.

Analysis of Intrinsic Brain Connectivity among RSNs

The ICA algorithm assumes that the signal time courses of brain areas belonging to the same IC are synchronous [Calhoun et al., 2004]. Although RS components are spatially independent, significant temporal correlations exist between them. We explored such temporal associations by analyzing the time series of the RSNs of interest using the FNC toolbox (http://mialab.mrn.org), and computing a constrained maximal lagged correlation between component time courses as described previously [Jafri et al., 2008]. The maximum allowed lag between time courses was set at 6 s. The time courses from all ICs of interest and for all subjects were interpolated, using low-pass temporal interpolation implemented in Matlab (The MathWorks, Natick, MA) and resampled to 250-ms bins to enable the detection of sub-TR hemodynamic delay differences between subjects [Calhoun et al., 2000; Jafri et al., 2008]. Subsequently, the maximal lagged correlation was examined among all pair-wise combinations between components. In other words, we examined the correlation between two IC time courses, A and B, when B is circularly shifted from -6 to $+6$ s around A. The maximal correlation value and the corresponding lag were saved for each of the analyzed time course pairs.

Structural MRI Analysis

Following standard procedures in our lab, [Rocca et al., 2012] lesion volumes (LVs) were measured from the dual-echo scans (Jim 5.0, Xinapse Systems, www.xinapse.com). For the analysis of white matter and gray matter (GM) volumes, 3D FFE images were segmented using SPM8 and the "New Segment" toolbox. The algorithm used by this toolbox for segmentation is based on the maximum likelihood mixture model [Ashburner and Friston, 1997] and, thanks to the

use of improved registration models and of an extended set of tissue probability maps, is able to produce more accurate maps of the CSF than those produced by the classical SPM segmentation. After producing mutually exclusive masks of white matter, GM, and CSF tissues, the intracranial volume (ICV) was calculated as the sum of white matter, GM, and CSF volumes. Then, brain parenchymal fraction (BPF) (white matter + GM volumes [GMVs]/ICV), GM fraction (GMF) (GMV/ICV), and white matter fraction (white matter volume/ICV) were calculated. To exclude a possible influence of GM atrophy on the voxel-wise comparisons of RS FC between healthy controls and pediatric RRMS patients, the average *Z*-scores of GMV were extracted from each cluster of each RSN of interest and used as a confounding covariate in the statistical analysis as described previously [Villain et al., 2008]. Briefly, the GM maps obtained by segmenting 3D FFE images were spatially normalized to the GM population-specific template generated from the complete image set by using the Diffeomorphic Anatomical Registration using Exponentiated Lie algebra (DARTEL) registration method [Ashburner, 2007] and smoothed using a 6-mm Gaussian kernel (the same as used to smooth RS fMRI scans). The resulting GM maps were used to create *Z*-score maps of GM atrophy by applying the following formula: ([subject individual GM value − control mean GM value]/control [SD] GM value) as described previously [Villain et al., 2008].

Diffusion weighted images were first corrected for distortion induced by eddy currents, using an algorithm which maximizes the mutual information between the diffusion un-weighted and the weighted images [Studholme et al., 1996]. Then, the DT was calculated, and mean diffusivity (MD) and fractional anisotropy (FA) derived for every pixel as described previously [Cercignani et al., 2001]. The $b = 0$ image of the PGSE acquisition was coregistered with the *T*2-weighted images and the same transformation applied to the DT-derived maps as described previously [Absinta et al., 2010]. Using SPM8, brain GM, white matter, and CSF were automatically segmented from dual-echo images. The resulting masks were superimposed onto the MD and FA maps (on which hyperintense lesions were masked out previously), and the corresponding MD and FA histograms of the normal-appearing white matter and GM were produced. For each histogram, the average MD and FA were measured.

Statistical Analysis

A nonparametric Mann–Whitney *U*-test was used to assess between-group differences in clinical and MRI measures using the SPSS software package. Comparisons among controls, CP, and CI MS patients were performed by using a Kruskall and Wallis test. Individual subjects' data from all RSNs of interest were entered into the SPM8 random-effect analysis, to assess the spatial extent of within-group FC (one-sample *t*-test in controls and MS patients together, $P < 0.05$; family-wise error corrected; cluster extent = 50 voxels). The mean RS FC within each RSN was computed by averaging the *Z*-scores of a given RSN for each study subject. Regional *Z*-scores of RS FC and the corresponding regional *Z*-scores of GMV were extracted from each significant SPM cluster of each network using the Marsbar toolbox [Brett et al., 2002]. Average FC values of whole RSN and regional FC values of each SPM cluster were compared between controls and pediatric MS patients, as well as among controls, CP, and CI MS patients, using SPSS with ANOVA models adjusted for age, gender, and average mean motion. For each network, a correction for multiple comparisons was performed using false discovery rate (FDR) [Benjamini and Hochberg, 1995]. Correlations between RS abnormalities (i.e., *Z*-scores of the clusters showing significant differences between groups) versus disease duration, EDSS, T2 LV, and DT MRI metrics were assessed using multiple regression models adjusted for age and gender. The whole analysis was also repeated after adding the regional *Z*-scores of GMV as a covariate (or the GMF for the comparison of whole RSN FC).

Correlations and lag values obtained for each subject with the FNC toolbox were averaged for the two groups. Statistically significant within-group correlations among RSNs were calculated for each group, separately, using one-sample *t*–tests. Between-group differences of FNC were then assessed using a two-sample *t*-test (when comparing controls vs. all pediatric MS patients) and an ANOVA model (when comparing controls, CP, and CI MS patients). As for RS FC analysis, correction for multiple comparison was performed by using FDR, as implemented in the FNC toolbox [Jafri et al., 2008]. As it was the case for FC, FNC analysis was also repeated after adding the GMF as a confounding covariate.

RESULTS

Structural MRI

Table I summarizes the main structural MRI characteristics of the study groups. Results of the neuropsychological assessment showed that 25 pediatric MS patients were CP. Controls, CP, and CI MS patients were matched for gender and age (Table I). Compared to controls, pediatric MS patients had a reduced normal-appearing white matter average FA and increased GM MD, whereas no between-group differences were found for BPF, GMF, white matter fraction, normal-appearing white matter MD, and GM FA. Compared to CP patients, pediatric CI MS patients had longer disease duration, lower normal-appearing white matter average FA, and higher GM MD (Table I).

Intrinsic Brain Activity in RS Networks

The analysis of RS fMRI detected 11 spatial maps of potentially relevant RSNs, including those related to

TABLE II. Mean values of *Z*-scores (and SDs) of global RS functional connectivity within each RS network of interest in healthy controls and pediatric patients with MS, first considered as a whole and then divided into CP and CI patients

RS networks	Healthy controls	Pediatric MS patients	CP MS patients	CI MS patients	*P*-value[a]	*P*-value[b]	*P*-value[c]	*P*-value[d]
Sensorimotor network I	1.11 (0.20)	1.11 (0.18)	1.11 (0.21)	1.13 (0.20)	0.76	0.69	0.73	0.82
Sensorimotor network II	1.83 (0.27)	1.81 (0.30)	1.82 (0.26)	1.78 (0.39)	0.82	0.66	0.87	0.96
Primary visual network	1.40 (0.37)	1.43 (0.37)	1.43 (0.35)	1.43 (0.38)	0.63	0.46	0.65	0.58
Secondary visual network	1.03 (0.23)	1.05 (0.23)	1.05 (0.25)	1.06 (0.18)	0.74	0.86	0.94	0.96
Auditory network	1.51 (0.20)	1.52 (0.19)	1.50 (0.20)	1.53 (0.20)	0.91	0.46	0.60	0.73
Default mode network	0.41 (0.09)	0.39 (0.11)	0.40 (0.11)	0.39 (0.10)	0.33	0.56	0.76	0.85
Executive control network	0.95 (0.16)	0.92 (0.17)	0.96 (0.16)	0.86 (0.18)	0.36	0.79	0.11	0.38
Salience network	1.16 (0.16)	1.13 (0.19)	1.14 (0.18)	1.08 (0.21)	0.40	0.89	0.53	0.61
Parietal attention network	0.99 (0.16)	1.02 (0.12)	1.03 (0.14)	1.02 (0.09)	0.46	0.46	0.76	0.86
Working memory network (left)	0.83 (0.13)	0.83 (0.12)	0.84 (0.11)	0.80 (0.10)	0.90	0.53	0.72	0.83
Working memory network (right)	0.94 (0.14)	0.97 (0.12)	0.98 (0.11)	0.95 (0.14)	0.58	0.52	0.74	0.73

[a]Comparison between healthy controls and all pediatric MS patients; ANOVA model adjusted for age, gender, and average mean motion.
[b]Comparison between healthy controls and all pediatric MS patients; ANOVA model adjusted for age, gender, average mean motion, and GMF.
[c]Comparison among healthy controls, CP, and CI pediatric MS patients; ANOVA model adjusted for age, gender, and average mean motion.
[d]Comparison among healthy controls, CP, and CI pediatric MS patients; ANOVA model adjusted for age, gender, average mean motion, and GMF.

sensorimotor areas (sensorimotor RSN I and II, R^2 with the sensorimotor network template = 0.34 and 0.23), primary, and secondary visual cortical areas (R^2 with the primary and secondary visual networks templates = 0.62 and 0.46), primary and secondary auditory areas (R^2 with the auditory network template = 0.59), DMN (R^2 with the DMN template = 0.35), ECN (R^2 with the ECN template = 0.52), SN (R^2 with the SN template = 0.25), two WMNs (R^2 with the templates of the left and right WMN = 0.28 for both networks), and one frontoparietal network related to attention (R^2 with the attention RSN template = 0.20). All these components were stable across multiple runs of IC decomposition (stability index assessed by ICASSO ranged from 0.93 to 0.97).

Table II summarizes the mean FC values (expressed as *Z*-scores) of each RSN in healthy controls and pediatric MS patients, first considered as a whole and then divided into CP and CI MS patients. No differences were found among study groups, even after adjusting for GMF.

Table III and Figure 1 summarize and show the regional differences between healthy controls and pediatric MS patients (as a whole and divided into CP and CI MS patients) for the RSNs identified. Compared to controls, pediatric MS patients had a decreased FC of several regions of the sensorimotor networks (R postcentral gyrus and L cerebellum), secondary visual network (L vermis of the cerebellum), DMN (L angular gyrus), ECN (L middle temporal gyrus [MTG]), and bilateral WMN (L and R precuneus). They also experienced an increased FC in the R medial frontal gyrus of the attention network (Table III). The majority of these between-group differences remained significant after adjusting for regional GMV (Table III). Significant differences between controls, CP, and CI MS patients were found for RS FC of the sensorimotor network (L cerebellum, $P = 0.003$), DMN (L angular gyrus, $P = 0.01$), and L WMN (R precuneus, $P = 0.02$). Only RS FC of this latter cluster was significantly different between pediatric CP and CI MS patients at post hoc comparison (Table III).

Intrinsic Brain Connectivity among RS Networks

FNC results are summarized in Table IV, which reports significant correlations found among RSNs in healthy controls and pediatric MS patients, separately, and significant differences of correlations between groups. Compared to controls, pediatric MS patients had an increased FC between the sensorimotor II network and the DMN ($P = 0.01$), and between the L WMN and the attention network ($P = 0.01$). They also showed a decreased FC between the L WMN and the DMN ($P = 0.02$). The decreased FC between L WMN and DMN was the only difference surviving to the correction for GM atrophy ($P = 0.01$). No differences of FNC were found between CP and CI MS patients (data not shown). The lag of correlations among RSNs also did not differ between groups.

Analysis of Correlations

In pediatric MS patients, T2 LV was significantly correlated with increased FC of the R medial frontal gyrus ($r = -0.46$, $P = 0.003$) (Fig. 2) of the attention network. This correlation also remained significant when excluding the

TABLE III. Mean values of *Z*-scores (and SD) of RS FC within the clusters showing a significant difference between healthy controls and patients with pediatric MS, first considered as a whole and then divided into CP and CI patients

RSNs	Cluster	MNI space coordinates *x y z*	Healthy controls	Pediatric MS patients	CP MS patients	CI MS patients	*P*-value[a]	*P*-value[b]	*P*-value[c]	*P*-value[d]
Sensorimotor II	L cerebellum (lobule VI)	−18 −64 −26	1.03 (0.38)	0.70 (0.39)	0.72 (0.41)	0.63 (0.40)	0.001*	0.001*	0.4	0.5
	R postcentral gyrus (BA2)	57 −31 30	0.70 (0.37)	0.51 (0.39)	0.50 (0.43)	0.55 (0.32)	0.05	0.08	0.4	0.4
Secondary visual network	L cerebellum (vermis)	−3 −55 −18	0.81 (0.64)	0.43 (0.53)	0.45 (0.52)	0.47 (0.48)	0.01*	0.06	0.8	0.7
DMN	L angular gyrus (BA39)	−45 −70 34	1.02 (0.66)	0.61 (0.52)	0.62 (0.52)	0.64 (0.51)	0.002*	0.006	0.5	0.2
ECN	L MTG (BA37)	−63 −52 −6	0.66 (0.36)	0.49 (0.36)	0.45 (0.34)	0.52 (0.41)	0.05	0.05	0.6	0.4
Fronto-parietal attention network	**R medial frontal gyrus (BA8)**	**3 23 50**	**0.72 (0.63)**	**0.95 (0.41)**	0.99 (0.39)	0.92 (0.48)	**0.05**	**0.3**	0.8	0.9
WMN (L)	R precuneus (BA7)	9 −64 66	0.85 (0.42)	0.66 (0.38)	0.76 (0.34)	0.49 (0.41)	0.04	0.05	0.05	0.05
WMN (R)	L precuneus (BA5)	−3 −52 58	0.76 (0.34)	0.63 (0.22)	0.64 (0.23)	0.58 (0.23)	0.04	0.01	0.3	0.5

[a]ANOVA model adjusted for age, gender, and average mean motion; **P*-values surviving to the FDR correction for multiple comparisons.
[b]ANOVA model adjusted for age, gender, average mean motion, and *Z*-score of regional GM volume; **P*-values surviving to the FDR correction for multiple comparisons.
[c]ANOVA model adjusted for age, gender, and average mean motion (significance at post hoc comparison between CP and CI patients).
[d]ANOVA model adjusted for age, gender, average mean motion, and *Z*-score for regional GM volume (significance at post hoc comparison between CP and CI patients).
Clusters with increased RS FC in pediatric MS patients versus healthy controls are identified in bold font.
Abbreviations: L, left; R, right; RS, resting state; MS, multiple sclerosis; MNI, Montreal Neurological Institute; DMN, default mode network; ECN, executive control network; SN, salience network; WMN, working memory network; BA, Brodmann area; MTG, middle temporal gyrus.

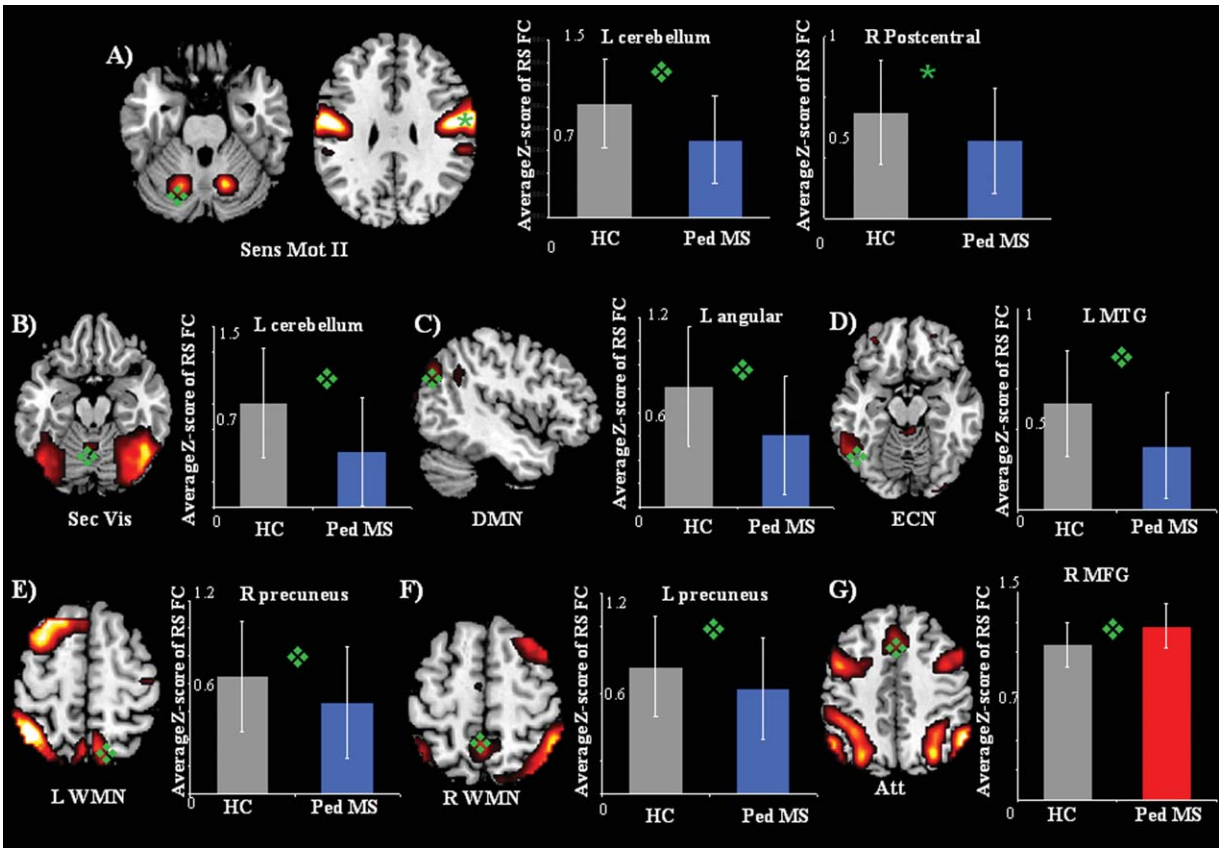

Figure 1.

Illustrative examples of the spatial patterns of RS FC from healthy controls and pediatric MS patients ($P < 0.05$, family-wise error corrected) and bar plots showing average *Z*-scores and standard deviations of each significant cluster of between-group difference. (**A**) Sensorimotor network II; (**B**) secondary visual network; (**C**) DMN; (**D**) ECN; (**E**) left (L) WMN; (**F**) right (R) WMN; (**G**) frontoparietal attention network. Blue bars represent clusters of decreased RS FC in pediatric MS patients versus controls, and red bars represent clusters of increased RS FC in pediatric MS patients versus controls. Abbreviations: L, left; R, right; MTG, middle temporal gyrus; MFG, medial frontal gyrus.

three outlier patients having a T2 LV of >10 mL ($r = -0.32$, $P = 0.05$). No correlations were found between RS FC modifications and EDSS, disease duration, and normal-appearing white matter and GM DT MRI values. Similarly, no correlations were detected between FNC correlation coefficient and clinical and structural MRI variables.

DISCUSSION

Using a task-free and unbiased analysis, in this observational study, we quantified abnormalities of FC within and between the principal brain RSNs in a relatively large group of pediatric RRMS patients with a range of disabilities and disease durations, with the ultimate goal of describing FC modifications in this population, their correlation with clinical manifestations (disability and cognitive impairment), and their modulation by structural brain damage.

Studies in adult patients with MS have demonstrated abnormal RS FC of several sensory and cognitive networks through the course of the disease, starting from patients with clinically isolated syndromes (CIS) suggestive of MS [Roosendaal et al., 2010] to those with the progressive disease clinical phenotypes [Rocca et al., 2010b]. However, these studies did not provide univocal results, leading to somewhat discordant interpretations of the role of RS FC modifications in these patients. Specifically, although some investigations found a distributed increased global FC of the main brain RSN [Faivre et al., 2012; Roosendaal et al., 2010], others did not [Rocca et al., 2012]. Several factors may help to explain these discrepancies between the previous studies, including methodological aspects related to RS analysis, network selection, and clinical and neuropsychological scales administered, heterogeneity of clinical

TABLE IV. Within-group correlation coefficients (*r*) among RSNs with potential functional relevance in healthy controls and pediatric patients with MS assessed with FNC analysis

RSN pair: correlation		Controls		Pediatric MS patients		
Between	And	*R*-value	*P*-value[b]	*R*-value	*P*-value[b]	*P*-value[a]
Sensorimotor I	Sensorimotor II	0.33	<0.001*	0.40	<0.001*	n.s.
	Primary visual	0.43	<0.001*	0.40	<0.001*	n.s.
	Secondary visual	0.32	<0.001*	0.31	<0.001*	n.s.
	Auditory	0.49	<0.001*	0.42	<0.001*	n.s.
	DMN	0.24	<0.001*	0.27	<0.001*	n.s.
	SN	0.20	<0.001*	—	n.s.	n.s.
Sensorimotor II	Primary visual	0.24	<0.001*	0.32	<0.001*	n.s.
	Secondary visual	0.23	0.002*	0.32	<0.001*	n.s.
	Auditory	0.44	<0.001*	0.44	<0.001*	n.s.
	DMN	**—**	**n.s.**	**0.21**	**<0.001***	**0.01**
	SN	0.10	0.03	—	n.s.	n.s.
	WMN (R)	—	n.s.	−0.12	0.005*	n.s.
	Frontoparietal attention	0.21	<0.001*	0.12	0.02*	n.s.
Primary visual	Secondary visual	0.36	<0.001*	0.38	<0.001*	n.s.
	Auditory	0.38	<0.001*	0.36	<0.001*	n.s.
	DMN	0.23	<0.001*	0.24	<0.001*	n.s.
	SN	0.23	0.001*	0.15	0.001*	n.s.
	WMN (L)	0.12	0.02	0.13	0.008*	n.s.
	Frontoparietal attention	0.17	0.005*	0.20	<0.001*	n.s.
Secondary visual	Auditory	0.31	<0.001*	0.30	<0.001*	n.s.
	DMN	—	n.s.	0.12	0.01*	n.s.
	SN	—	n.s.	−0.11	0.01*	n.s.
	WMN (R)	—	n.s.	−0.09	0.04	n.s.
	Frontoparietal attention	0.17	0.01*	0.17	0.002*	n.s.
Auditory	ECN	0.24	<0.001*	0.21	<0.001*	n.s.
	SN	0.43	<0.001*	0.35	<0.001*	n.s.
	WMN (L)	−0.17	0.009*	−0.24	<0.001*	n.s.
	WMN (R)	—	n.s.	−0.17	<0.001*	n.s.
	Frontoparietal attention	0.37	<0.001*	0.28	<0.001*	n.s.
DMN	ECN	—	n.s.	−0.12	0.04	n.s.
	SN	—	n.s.	−0.13	0.01*	n.s.
	WMN (L)	**0.44**	**<0.001***	**0.33**	**<0.001***	**0.02**
	WMN (R)	0.24	<0.001*	0.20	<0.001*	n.s.
ECN	SN	0.65	<0.001*	0.63	<0.001*	n.s.
	WMN (R)	0.30	<0.001*	0.23	<0.001*	n.s.
	Frontoparietal attention	0.37	<0.001*	0.25	<0.001*	n.s.
SN	Parietal attention	0.39	<0.001*	0.37	<0.001*	n.s.
	WMN (R)	0.29	<0.001*	0.30	<0.001*	n.s.
WMN (L)	**Frontoparietal attention**	**0.13**	**0.02**	**0.29**	**<0.001***	**0.01**
	WMN (R)	0.33	<0.001*	0.35	<0.001*	n.s.
WMN (R)	Frontoparietal attention	0.34	<0.001*	0.30	<0.001*	n.s.

[a]Two-sample *t*-test, *P*-values uncorrected for multiple comparison.
[b]One-sample *t*-test, *P*-values uncorrected for multiple comparison.
**P*-values surviving FDR correction for multiple comparisons.
Significant between-group connectivity differences, as well as connectivities significantly present in only one group, are highlighted in bold font. Note that as coefficients are symmetrical (i.e., given two RSNs *A* and *B*, correlation between *A* and *B* is the same as that between *B* and *A*), they were reported only once.
Abbreviations: DMN, default mode network; ECN, executive control network; SN, salience network; WMN, working memory network; L, left; R, right; n.s., not significant.

characteristics of the patients enrolled and the severity of structural damage to the CNS. Notably, in some studies the regional analysis of RS FC abnormalities showed a reduced FC in clinically and/or CI patients [Bonavita et al., 2011; Rocca et al., 2012, 2010b], which has been interpreted as a failure of compensatory mechanisms owing to accumulation of structural disease burden. In the same studies, an increased FC has been interpreted as

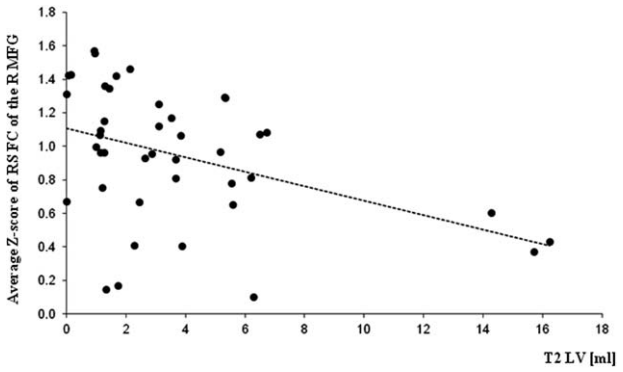

Figure 2.

Scatterplot of the correlation between *T*2 LV and average *Z*-score of RS FC of the right (R) MFG of the attention network. Note that the correlation also remained significant when excluding the three outlier patients having a *T*2 LV of >10 mL ($r = -0.32$, $P = 0.05$).

reflecting a compensatory effect [Bonavita et al., 2011; Roosendaal et al., 2010] as it was found in patients with CIS but not in those with RRMS [Bonavita et al., 2011; Roosendaal et al., 2010], and was more evident in cognitively intact patients [Bonavita et al., 2011; Roosendaal et al., 2010]. Such a straightforward compensation hypothesis has been recently contradicted by the demonstration that increased RS FC in early-stage MS patients of areas involved in attention and cognitive control correlated with a poorer clinical and cognitive performance [Faivre et al., 2012; Hawellek et al., 2011]. As a consequence, against the prevailing compensatory theory, it has been proposed that increased RS FC abnormalities might also reflect maladaptive mechanisms, which may contribute to impaired cognitive functions.

The study of patients with pediatric MS offers the unique opportunity to examine disease-related mechanisms of damage and recovery operative in a different stage of the disease. Using ICA, we identified 11 potentially relevant RSNs both in pediatric controls and in pediatric patients. In line with the results of a few recent studies in adult patients with RRMS [Rocca et al., 2012; Roosendaal et al., 2010], the analysis of global network RS FC revealed no differences between patients and controls. Conversely, the regional analysis of intranetwork RS FC showed that, with the exception of the primary visual, auditory, and SN, for all the remaining networks significant differences existed between controls and pediatric RRMS patients. In detail, compared to controls, pediatric RRMS patients had a decreased RS FC of several areas of sensory- and cognitive-related RSNs, mainly located in posterior brain regions (within the parietal, temporal, and occipital lobes). Regional abnormalities of RS FC of the principal brain networks have been consistently demonstrated in the majority of neurological and psychiatric diseases of adulthood and childhood [Greicius et al., 2007; Seeley et al., 2007; van den Heuvel and Hulshoff Pol, 2010; Zhou et al., 2010]. However, it is still matter of debate whether such abnormalities are a primary cause of symptoms in these conditions, or arise secondary to common etiologic mechanisms.

The between-group comparison also showed that, compared to controls, pediatric MS patients had an increased RS FC of the medial frontal gyrus (of the attention network), which was inversely related to the volume of *T*2 lesions. Notably, such an increased RS FC was more pronounced (even if this was not statistically significant) in CP MS patients. Although caution is needed when interpreting this finding, also in consideration of the fact that such a difference was not detected after correction for GMV, the correlation we found suggests that this increased RS FC might, at least partially, contribute to counteract disease-related abnormalities when structural damage is relatively modest, whereas this mechanism is likely to fail with accumulating structural abnormalities. Although this hypothesis has to be confirmed by future RS FC studies, results obtained by previous RS fMRI studies seem to support the occurrence of this mechanism: in adult patients with MS, increased RS FC of several regions has been interpreted as an indication of an early but finite process as it was detected in CIS patients without structural damage, but not in RRMS patients with widespread white matter abnormalities [Roosendaal et al., 2010]. Similarly, in healthy adults, an increased RS FC in the DMN has been demonstrated in APOE ε4 carriers relative to noncarriers [Filippini et al., 2009; Westlye et al., 2011], suggesting that these measures might be sensitive to disease-related abnormalities that occur years before the progression of clinical symptoms. The question of whether such an increased RS FC in a given brain network in pediatric MS patients might protect against the onset of clinical deficits or, conversely, may confer a systematic vulnerability to such a network can only be addressed by longitudinal studies.

In our study, RS FC abnormalities in pediatric MS patients did not correlate with damage to the normal-appearing white matter and GM. The absence of such a correlation might be owing from the one hand to the relatively modest structural damage to the CNS usually detected in pediatric MS patients when compared to their adult counterpart, and from the other to the relatively global approach we applied to quantify such a damage. In this perspective, we cannot exclude that the use of a regional method to define the distribution of damage in the different brain compartments would have allowed us to highlight the critical role of some strategic structures (e.g., the thalamus) for the observed RS FC abnormalities.

The pattern of RS FC abnormalities we have found in pediatric MS patients (reduced FC mostly located in posterior brain regions and increased FC in anterior brain regions) differs from what has been previously described in adult patients with MS, in whom areas of increased and decreased FC were unevenly distributed across the brain hemispheres [Rocca et al., 2012]. An important factor that

should be considered when analyzing these disparities, in addition to differences in clinical and structural MRI features between pediatric and adult patients (which may account for a regional heterogeneity of functional abnormalities), is the level of maturation of a given network or of specific brain regions, which could result in different vulnerability to the disease processes. Indeed, maturation of large-scale brain networks is characterized by a weakening of short-range FC and a strengthening of long-range FC [Fair et al., 2007; Supekar et al., 2009]. In addition, children's brains have a less hierarchical organization than young adults [Supekar et al., 2009]. Therefore, we cannot exclude the possibility that our findings in pediatric MS patients are owing to a deficit in the development of large-scale brain connectivity, with an impaired shift from stronger short-range connections to stronger long-range connections. This might also explain the fairly modest differences of internetwork connectivity we detected between patients and controls. Again, whether this protects these patients or makes them more vulnerable to disease progression needs to be assessed by a longitudinal evaluation. So far, it has been postulated that lower levels of hierarchical organization in children may be protective, allowing greater flexibility in network reconfiguration on the basis of individual experience [Supekar et al., 2009]. It is worth mentioning that, similarly to what we have previously found in adult patients with RRMS [Rocca et al., 2012], also in pediatric patients affected by this condition the analysis of internetwork connectivity showed a distributed abnormality of communication among the principal brain RSN, which is probably owing to the uneven distribution of structural damage to the CNS, which is a typical finding in this condition.

Globally, our results point toward the presence of diffuse abnormalities of large-scale neuronal network connectivity in patients with pediatric MS, which might result, at least partially, from a deficit of maturation of their functional interactions. A longitudinal evaluation is now required to determine whether the increased FC we found in some core regions of these networks may help to limit the clinical consequences of the disease or, conversely, reflect a maladaptive mechanism making these regions more vulnerable to damage.

CONFLICT OF INTEREST

Maria A. Rocca received speakers honoraria from Biogen Idec and Serono Symposia International Foundation and receives research support from the Italian Ministry of Health.

Paola Valsasina, Martina Absinta, Lucia Moiola, Pierangelo Veggiotti, and Andrea Falini report no conflict of interest.

Angelo Ghezzi has served on scientific advisory boards for Merck Serono, Biogen Idec Teva Pharmaceutical Industries Ltd., has received speaker honoraria from Merck Serono, Biogen Idec, Bayer Schering Pharma, and Novartis, Serono Symposia International; served as a consultant for Novartis; and receives research support from Sanofi-Aventis, Biogen Idec, and Merck Serono.

Maria Pia Amato has received personal compensation from Merck Serono, Biogen, Bayer Schering, Genzyme, Teva, and Novartis for serving on scientific advisory board and for speaking, and has received financial support for research activities from Merck Serono, Biogen Idec, Bayer Schering, Genzyme, Novartis, Genzyme, and Teva.

Mark A. Horsfield has acted as a consultant to Biogen Idec and to GE Healthcare, and is a stock holder of Xinapse Systems.

Giancarlo Comi has received compensation for consulting services and/or speaking activities from Novartis, Teva Pharmaceutical Ind., Sanofi, Genzyme, Merck Serono, Biogen Bayer, Actelion, and Serono Symposia International Foundation.

Massimo Filippi serves on scientific advisory boards for Teva Pharmaceutical Industries and Genmab A/S; has received received compensation for consulting services and/or speaking activities from Bayer Schering Pharma, Biogen Idec, Genmab A/S, Merck Serono, and Teva Pharmaceutical Industries; and receives research support from Bayer Schering Pharma, Biogen Idec, Genmab A/S, Merck Serono, Teva Pharmaceutical Industries, Italian Ministry of Health, Fondazione Italiana Sclerosi Multipla, Cure PSP, and the Jacques and Gloria Gossweiler Foundation (Switzerland).

REFERENCES

Absinta M, Rocca MA, Moiola L, Ghezzi A, Milani N, Veggiotti P, Comi G, Filippi M (2010): Brain macro- and microscopic damage in patients with paediatric MS. J Neurol Neurosurg Psychiatry 81:1357–1362.

Absinta M, Rocca MA, Moiola L, Copetti M, Milani N, Falini A, Comi G, Filippi M (2011): Cortical lesions in children with multiple sclerosis. Neurology 76:910–913.

Ashburner J (2007): A fast diffeomorphic image registration algorithm. Neuroimage 38:95–113.

Ashburner J, Friston K (1997): Multimodal image coregistration and partitioning—A unified framework. Neuroimage 6:209–217.

Banwell B, Ghezzi A, Bar-Or A, Mikaeloff Y, Tardieu M (2007): Multiple sclerosis in children: Clinical diagnosis, therapeutic strategies, and future directions. Lancet Neurol 6:887–902.

Bell AJ, Sejnowski TJ (1995): An information-maximization approach to blind separation and blind deconvolution. Neural Comput 7:1129–1159.

Benjamini Y, Hochberg Y (1995): Controlling the false discovery rate: A practical and powerful approach to multiple testing. J R Stat Soc Ser B 57:289–300.

Bonavita S, Gallo A, Sacco R, Corte MD, Bisecco A, Docimo R, Lavorgna L, Corbo D, Costanzo AD, Tortora F, Cirillo M, Esposito F, Tedeschi G (2011): Distributed changes in default-mode resting-state connectivity in multiple sclerosis. Mult Scler 17:411–422.

Brett M, Anton J-L, Valabregue R, Poline JP (2002): Region of interest analysis using an SPM toolbox. NeuroImage 16:372.

Calhoun V, Adali T, Kraut M, Pearlson G (2000): A weighted least-squares algorithm for estimation and visualization of relative latencies in event-related functional MRI. Magn Reson Med 44:947–954.

Calhoun VD, Adali T, Pearlson GD, Pekar JJ (2001): A method for making group inferences from functional MRI data using independent component analysis. Hum Brain Mapp 14:140–151.

Calhoun VD, Kiehl KA, Liddle PF, Pearlson GD (2004): Aberrant localization of synchronous hemodynamic activity in auditory cortex reliably characterizes schizophrenia. Biol Psychiatry 55: 842–849.

Cercignani M, Bozzali M, Iannucci G, Comi G, Filippi M (2001): Magnetisation transfer ratio and mean diffusivity of normal appearing white and grey matter from patients with multiple sclerosis. J Neurol Neurosurg Psychiatry 70:311–317.

Chabas D, Ness J, Belman A, Yeh EA, Kuntz N, Gorman MP, Strober JB, De Kouchkovsky I, McCulloch C, Chitnis T, Rodriguez M, Weinstock-Guttman B, Krupp LB, Waubant E; US Network of Pediatric MS Centers of Excellence (2010): Younger children with MS have a distinct CSF inflammatory profile at disease onset. Neurology 74:399–405.

Dale RC, Brilot F, Banwell B (2009): Pediatric central nervous system inflammatory demyelination: Acute disseminated encephalomyelitis, clinically isolated syndromes, neuromyelitis optica, and multiple sclerosis. Curr Opin Neurol 22:233–240.

Damoiseaux JS, Rombouts SA, Barkhof F, Scheltens P, Stam CJ, Smith SM, Beckmann CF (2006): Consistent resting-state networks across healthy subjects. Proc Natl Acad Sci USA 103: 13848–13853.

Fair DA, Dosenbach NU, Church JA, Cohen AL, Brahmbhatt S, Miezin FM, Barch DM, Raichle ME, Petersen SE, Schlaggar BL (2007): Development of distinct control networks through segregation and integration. Proc Natl Acad Sci USA 104:13507–13512.

Faivre A, Rico A, Zaaraoui W, Crespy L, Reuter F, Wybrecht D, Soulier E, Malikova I, Confort-Gouny S, Cozzone PJ, Pelletier J, Ranjeva JP, Audoin B (2012): Assessing brain connectivity at rest is clinically relevant in early multiple sclerosis. Mult Scler 18:1251–1258.

Filippini N, MacIntosh BJ, Hough MG, Goodwin GM, Frisoni GB, Smith SM, Matthews PM, Beckmann CF, Mackay CE (2009): Distinct patterns of brain activity in young carriers of the APOE-epsilon4 allele. Proc Natl Acad Sci USA 106:7209–7214.

Fox MD, Snyder AZ, Vincent JL, Corbetta M, Van Essen DC, Raichle ME (2005): The human brain is intrinsically organized into dynamic, anticorrelated functional networks. Proc Natl Acad Sci USA 102:9673–9678.

Franco AR, Pritchard A, Calhoun VD, Mayer AR (2009): Interrater and intermethod reliability of default mode network selection. Hum Brain Mapp 30:2293–2303.

Ghassemi R, Antel SB, Narayanan S, Francis SJ, Bar-Or A, Sadovnick AD, Banwell B, Arnold DL (2008): Lesion distribution in children with clinically isolated syndromes. Ann Neurol 63:401–405.

Greicius MD, Flores BH, Menon V, Glover GH, Solvason HB, Kenna H, Reiss AL, Schatzberg AF (2007): Resting-state functional connectivity in major depression: Abnormally increased contributions from subgenual cingulate cortex and thalamus. Biol Psychiatry 62:429–437.

Hawellek DJ, Hipp JF, Lewis CM, Corbetta M, Engel AK (2011): Increased functional connectivity indicates the severity of cognitive impairment in multiple sclerosis. Proc Natl Acad Sci USA 108:19066–19071.

Himberg J, Hyvarinen A, Esposito F (2004): Validating the independent components of neuroimaging time series via clustering and visualization. Neuroimage 22:1214–1222.

Jafri MJ, Pearlson GD, Stevens M, Calhoun VD (2008): A method for functional network connectivity among spatially independent resting-state components in schizophrenia. Neuroimage 39: 1666–1681.

Jolles DD, van Buchem MA, Crone EA, Rombouts SA (2011): A comprehensive study of whole-brain functional connectivity in children and young adults. Cereb Cortex 21:385–391.

Krupp LB, Banwell B, Tenembaum S (2007): Consensus definitions proposed for pediatric multiple sclerosis and related disorders. Neurology 68:S7–S12.

Lublin FD, Reingold SC (1996): Defining the clinical course of multiple sclerosis: Results of an international survey. National Multiple Sclerosis Society (USA) Advisory Committee on Clinical Trials of New Agents in Multiple Sclerosis. Neurology 46: 907–911.

Maldjian JA, Laurienti PJ, Kraft RA, Burdette JH (2003): An automated method for neuroanatomic and cytoarchitectonic atlas-based interrogation of fMRI data sets. Neuroimage 19:1233–1239.

Muzik O, Chugani DC, Juhasz C, Shen C, Chugani HT (2000): Statistical parametric mapping: Assessment of application in children. Neuroimage 12:538–549.

Oldfield RC (1971): The assessment and analysis of handedness: The Edinburgh inventory. Neuropsychologia 9:97–113.

Portaccio E, Goretti B, Lori S, Zipoli V, Centorrino S, Ghezzi A, Patti F, Bianchi V, Comi G, Trojano M, Amato MP; Multiple Sclerosis Study Group of the Italian Neurological Society (2009): The brief neuropsychological battery for children: A screening tool for cognitive impairment in childhood and juvenile multiple sclerosis. Mult Scler 15:620–626.

Renoux C, Vukusic S, Mikaeloff Y, Edan G, Clanet M, Dubois B, Debouverie M, Brochet B, Lebrun-Frenay C, Pelletier J, Moreau T, Lubetzki C, Vermersch P, Roullet E, Magy L, Tardieu M, Suissa S, Confavreux C; Adult Neurology Departments KIDMUS Study Group (2007): Natural history of multiple sclerosis with childhood onset. N Engl J Med 356:2603–2613.

Rocca M, Valsasina P, Martinelli V, Misci P, Falini A, Comi G, Filippi M (2012): Large-scale neuronal network dysfunction in relapsing-remitting multiple sclerosis Neurology 79:1449–1457.

Rocca MA, Absinta M, Ghezzi A, Moiola L, Comi G, Filippi M (2009): Is a preserved functional reserve a mechanism limiting clinical impairment in pediatric MS patients? Hum Brain Mapp 30:2844–2851.

Rocca MA, Absinta M, Moiola L, Ghezzi A, Colombo B, Martinelli V, Comi G, Filippi M (2010a): Functional and structural connectivity of the motor network in pediatric and adult-onset relapsing-remitting multiple sclerosis. Radiology 254:541–550.

Rocca MA, Valsasina P, Absinta M, Riccitelli G, Rodegher ME, Misci P, Rossi P, Falini A, Comi G, Filippi M (2010b): Default-mode network dysfunction and cognitive impairment in progressive MS. Neurology 74:1252–1259.

Roosendaal SD, Schoonheim MM, Hulst HE, Sanz-Arigita EJ, Smith SM, Geurts JJ, Barkhof F (2010): Resting state networks change in clinically isolated syndrome. Brain 133:1612–1621.

Seeley WW, Menon V, Schatzberg AF, Keller J, Glover GH, Kenna H, Reiss AL, Greicius MD (2007): Dissociable intrinsic connectivity networks for salience processing and executive control. J Neurosci 27:2349–2356.

Simone IL, Carrara D, Tortorella C, Liguori M, Lepore V, Pellegrini F, Bellacosa A, Ceccarelli A, Pavone I, Livrea P

(2002): Course and prognosis in early-onset MS: Comparison with adult-onset forms. Neurology 59:1922–1928.

Smith SM, Fox PT, Miller KL, Glahn DC, Fox PM, Mackay CE, Filippini N, Watkins KE, Toro R, Laird AR, Beckmann CF (2009): Correspondence of the brain's functional architecture during activation and rest. Proc Natl Acad Sci USA 106: 13040–13045.

Studholme C, Hill DL, Hawkes DJ (1996): Automated 3-D registration of MR and CT images of the head. Med Image Anal 1: 163–175.

Supekar K, Musen M, Menon V (2009): Development of large-scale functional brain networks in children. PLoS Biol 7: e1000157.

Supekar K, Uddin LQ, Prater K, Amin H, Greicius MD, Menon V (2010): Development of functional and structural connectivity within the default mode network in young children. Neuroimage 52:290–301.

van den Heuvel MP, Hulshoff Pol HE (2010): Exploring the brain network: A review on resting-state fMRI functional connectivity. Eur Neuropsychopharmacol 20:519–534.

Villain N, Desgranges B, Viader F, de la Sayette V, Mezenge F, Landeau B, Baron JC, Eustache F, Chetelat G (2008): Relationships between hippocampal atrophy, white matter disruption, and gray matter hypometabolism in Alzheimer's disease. J Neurosci 28:6174–6181.

Westlye ET, Lundervold A, Rootwelt H, Lundervold AJ, Westlye LT (2011): Increased hippocampal default mode synchronization during rest in middle-aged and elderly APOE epsilon4 carriers: Relationships with memory performance. J Neurosci 31:7775–7783.

Zhou J, Greicius MD, Gennatas ED, Growdon ME, Jang JY, Rabinovici GD, Kramer JH, Weiner M, Miller BL, Seeley WW (2010): Divergent network connectivity changes in behavioural variant frontotemporal dementia and Alzheimer's disease. Brain 133:1352–1367.